Computers, Materials & Continua

Tech Science Press

https://doi.org/10.32604/cmc.2026.084488

ARTICLE

V2X-Enabled Parameter-Estimation-Based ILC for Repetitive Trajectory Tracking of Connected Vehicles under Trial-Varying Conditions

Ping Ma[1,2], **Quan Wang**[1,2] **and Yiyang Chen**[3,*]

[1]School of Internet of Things Engineering, Wuxi University, Wuxi, China
[2]Jiangsu Provincial University Key Laboratory of Vehicle-Road Multimodal Perception and Control, Wuxi University, Wuxi, China
[3]School of Mechanical and Electrical Engineering, Soochow University, Suzhou, China

*Corresponding Author: Yiyang Chen. Email: yychen90@suda.edu.cn

Received: 23 April 2026; Accepted: 01 July 2026; Published: 13 August 2026

ABSTRACT: Connected vehicles operating in V2X-enabled intelligent transportation systems often perform repetitive trajectory tracking in repeated tasks. In practical applications, traffic conditions, communication quality, and sensing accuracy may vary from trial to trial. These variations induce time-varying dynamics across repeated runs and reduce the effectiveness of iterative learning control (ILC) schemes when fixed or inaccurately identified models are used. To address this issue, this paper proposes a parameter-estimation-based ILC framework for connected vehicles. Parameter estimation is integrated with a norm-optimal ILC design through an expectation-maximization strategy. The time-varying model parameters and the learning input are updated iteratively. By exploiting the estimated parameter information at each trial, the proposed method improves tracking performance under random noise and trial-varying operating conditions. Convergence properties are analyzed for both noise-free and noisy cases. Comparative results demonstrate improved tracking accuracy and convergence performance over several benchmark methods.

KEYWORDS: Repetitive trajectory tracking; iterative learning control; parameter estimation

1 Introduction

Iterative learning control (ILC) is a learning-based control method for systems that perform repetitive tasks over a finite operation interval. Instead of relying only on feedback within a single run, ILC uses the input and tracking-error information obtained from previous trials to update the control signal for the next trial. Through this trial-to-trial correction mechanism, the output trajectory can be gradually improved. With the development of connected vehicles and vehicle-to-everything (V2X)-enabled intelligent transportation systems, repeated trajectory-tracking operations are increasingly involved in infrastructure-assisted driving, connected automated navigation, and cooperative transportation applications [1–3]. These application scenarios provide a suitable background for applying ILC to connected vehicle trajectory tracking.

Connected vehicle systems often operate under conditions that change with traffic flow, surrounding vehicle behavior, communication quality, and sensing accuracy. These factors may modify the effective system dynamics from one repeated run to another. Therefore, compared with time-invariant systems, connected vehicle trajectory tracking requires additional attention to model variation and parameter uncertainty. When the parameters related to vehicle motion and tracking behavior are not accurately known in advance, parameter estimation becomes an important tool for preserving control accuracy in dynamic transportation environments. Existing studies on parameter adaptation, collaborative perception, infrastructure-assisted vehicle operation, and lightweight traffic-scene detection have also indicated that the performance of networked transportation systems is closely related to real-time state acquisition and environment information [4–7].

Control and optimization of connected and automated vehicles have been widely studied under different traffic scenarios. For mixed traffic and infrastructure-constrained environments, trajectory planning and energy-efficient operation have received considerable attention. The work in [8] studied trajectory planning for connected and autonomous vehicles at freeway work zones under mixed traffic conditions. Eco-driving of connected autonomous vehicles in urban traffic networks with manually driven vehicle interactions was investigated in [9]. Platoon trajectory generation and distributed optimization for connected and automated vehicles were further considered in [10,11]. Recent studies have also considered resource allocation, vehicular edge computing, federated learning, and AoI-energy optimization in IoV and C-V2X-enabled networks [12–14]. These studies show that traffic, communication, computation, and sensing factors can strongly affect connected vehicle operation. However, most of the above works focus on planning, coordination, resource allocation, or energy optimization, while the trial-to-trial learning problem under varying system parameters is not their main concern.

ILC has also been extended to various time-varying and non-repetitive control problems. Related results include path-following control with trial-varying motion profiles, path-following performance optimization, event-triggered model-free adaptive learning, fuzzy adaptive consensus learning, and monotone convergence improvement with time-varying learning gains [15–17]. In addition, maximum-likelihood and auxiliary-model-based estimation methods have been developed for noisy, multivariate, nonlinear, and missing-data systems, which provides useful methodological support for parameter refinement under uncertain observations [18,19]. Machine-learning-based ILC, extreme-learning-machine-assisted ILC, parameter-estimation-based ILC, and indirect reference update frameworks have also been developed to reduce model mismatch and enhance tracking performance in non-repetitive time-varying systems [20–22]. Nevertheless, these methods are not specifically designed for connected vehicles affected simultaneously by traffic variation, communication fluctuation, and sensing uncertainty.

Motivated by the above observations, this work investigates repetitive trajectory tracking of connected vehicles under trial-varying traffic and communication conditions. The key difficulty lies in the mismatch between the actual time-varying system and the model used in the ILC update. If such mismatch exceeds the robustness range of a conventional fixed-model ILC scheme, tracking performance may deteriorate in networked transportation tasks. To address this problem, an expectation maximization (EM) estimation strategy is introduced into the learning process. The estimated time-varying parameters are used to update the lifted system representation, and the learning input is then computed based on the updated model information. Comparative studies are conducted to verify the effectiveness of the proposed method.

The main contributions of this work are summarized as follows:

(1) A parameter-estimation-based ILC framework is developed for repetitive trajectory tracking of connected vehicles under trial-varying traffic and communication conditions. Different from fixed-model ILC schemes, the proposed method updates the control input according to estimated time-varying parameters.
(2) An EM strategy is integrated into a norm-optimal ILC framework to realize iterative model refinement and learning-input adjustment. This design improves the adaptability of the controller to model mismatch and operating-condition variations.

(3) Convergence properties are established for both noise-free and noisy cases. Comparative results verify that the proposed method improves tracking accuracy and convergence performance in connected vehicle trajectory-tracking tasks.

Notation: $\mathbb{R}^n$ denotes the n-dimensional real vector space, and $\mathbb{R}^{m\times n}$ denotes the set of $m \times n$ real matrices. The inner product is denoted by $\langle\cdot,\cdot\rangle$, and the induced norm is denoted by $\|\cdot\|$ in a Hilbert space.

2 Problem Statement

This section establishes the modeling basis of the considered trajectory-tracking problem. The discrete-time time-varying dynamics are first introduced, followed by the parameter-estimation setting and the corresponding ILC tracking objective.

2.1 Time-Varying System Dynamics

The connected-vehicle tracking process is described by the following discrete-time linear time-varying model with stochastic perturbations:

$$\begin{cases} x_k(t+1) = \varphi_t x_k(t) + \theta_t u_k(t) + w \\ y_k(t) = \phi_t x_k(t) + v, \qquad t \in [0, N] \end{cases}, \tag{1}$$

where k denotes the trial index and t denotes the sampling instant within one trial. The vector $x_k(t) \in \mathbb{R}^n$ is the vehicle state vector, which describes the tracking-related motion states of the connected vehicle. The vector $u_k(t) \in \mathbb{R}^\ell$ is the control input applied to the vehicle motion system, and $y_k(t) \in \mathbb{R}^m$ is the measured output used for trajectory-tracking evaluation. The matrix $\varphi_t \in \mathbb{R}^{n\times n}$ is the time-varying state-transition matrix, $\theta_t \in \mathbb{R}^{n\times\ell}$ is the time-varying input matrix, and $\phi_t \in \mathbb{R}^{m\times n}$ is the time-varying output matrix. The process disturbance $w \in \mathbb{R}^n$ and the measurement noise $v \in \mathbb{R}^m$ describe the state perturbation and sensing uncertainty, respectively. They are modeled as $w \sim \mathbf{N}(0, W_t)$ and $v \sim \mathbf{N}(0, V_t)$, where $W_t \in \mathbb{R}^{n\times n}$ and $V_t \in \mathbb{R}^{m\times m}$ are the corresponding covariance matrices. The initial state prior is given by $x(0) \sim \mathbf{N}(x(0), P(0))$, with $x(0)$ and $P(0)$ known.

For the repeated tracking task, the initial state is reset to $x_k(0) = x_0$ at the beginning of each trial, as commonly required in ILC formulations. According to the lifted representation in [23], the input-output relation of the above system can be written as

$$y_k = G_k u_k + d_k + \varepsilon_k. \tag{2}$$

In the lifted representation, G_k denotes the lifted input-output operator that maps the stacked input sequence u_k to the stacked output sequence y_k over the finite trial horizon. The term d_k denotes the lifted bias term generated by the initial state and the time-varying state-transition dynamics. The term ε_k denotes the lifted noise or disturbance term, which collects the effects of process disturbance and measurement noise over one trial.

Because the model parameters vary with the sampling instant and may also change from trial to trial, the lifted operators G_k and d_k are not fixed. Following the construction in [24,25], they are given by

$$G_k = \begin{bmatrix} \phi_1\theta_0 & 0 & \cdots & 0 \\ \phi_2\varphi_1\theta_0 & \phi_2\theta_1 & \cdots & 0 \\ \vdots & \vdots & \ddots & \vdots \\ \phi_N \prod_{j=1}^{N-1} \varphi_j\theta_0 & \phi_N \prod_{j=2}^{N-1} \varphi_j\theta_1 & \cdots & \phi_N\theta_{N-1} \end{bmatrix}, \tag{3}$$

$$d_k = \left[(\phi_1\varphi_0)^T, \quad (\phi_2\varphi_1\varphi_0)^T, \quad \cdots, \quad (\phi_N \prod_{j=0}^{N-1} \varphi_j)^T \right]^T x_0, \tag{4}$$

$$\varepsilon_k = \nu + \begin{bmatrix} \phi_1 w \\ (\phi_2 + \phi_2\varphi_1)w \\ \vdots \\ (\phi_N \sum_{i=1}^{N} \prod_{j=i}^{N-1} \varphi_j)w \end{bmatrix}, \tag{5}$$

where $\phi_N \theta_{N-1} \neq 0$ is required for controllability. The main lifted variables in the above representation have the following dimensions: $G_k \in \mathbb{R}^{mN\times \ell N}$, $d_k \in \mathbb{R}^{mN}$, and $\varepsilon_k \in \mathbb{R}^{mN}$.

The stacked input and output vectors over one trial are defined as

$$u_k = [u_k(0), u_k(1), \cdots, u_k(N-1)]^T \in \mathbb{R}^{\ell N}, \tag{6}$$

$$y_k = [y_k(1), y_k(2), \cdots, y_k(N)]^T \in \mathbb{R}^{mN}. \tag{7}$$

The weighted norms used in the subsequent ILC design are introduced as

$$||u||_R^2 =< u, u >_R = u^T R u, ||y||_Q^2 =< y, y >_Q = y^T Q y, \tag{8}$$

where $R \in \mathbb{R}^{\ell N\times \ell N}$ and $Q \in \mathbb{R}^{mN\times mN}$ are symmetric positive definite weighting matrices.

2.2 *Time-Varying Parameter Estimation for Connected Vehicle Tracking*

In the considered connected-vehicle tracking problem, the relevant model parameters may change with traffic conditions, communication quality, and sensing accuracy. Parameter estimation is therefore introduced to update the model information by using data collected during repeated trials. These trial-varying effects may otherwise lead to model mismatch and reduce the effectiveness of learning control.

The estimation errors between the true and estimated parameter matrices are denoted by

$$||\varphi_t - \hat{\varphi}_t|| = \varkappa, \quad ||\theta_t - \hat{\theta}_t|| = \varsigma, \quad ||\phi_t - \hat{\phi}_t|| = \iota. \tag{9}$$

Assumption 1: *In repetitive trajectory-tracking tasks of connected vehicles under trial-varying traffic and communication conditions, the system dynamics change smoothly along the trials. The errors $\varkappa$, ς and ι are non-negative and sufficiently small so that $\lim_{k\to\infty} \varkappa = 0$, $\lim_{k\to\infty} \varsigma = 0$ and $\lim_{k\to\infty} \iota = 0$.*

In connected vehicle trajectory-tracking tasks, discrepancies commonly exist between the true parameter values and their estimates due to traffic variation, communication fluctuation, perception uncertainty, and vehicle operating condition changes. The engineering rationale of Assumption 1 is that the considered repetitive tracking task is performed on the same or similar route segment within a limited operating range. Therefore, the vehicle motion characteristics, communication quality, and sensing conditions usually vary gradually from one trial to the next rather than changing abruptly. The small-error condition reflects the availability of repeated input-output data for parameter refinement, while the convergence of $\varkappa$, ς, and ι represents the ideal case in which the estimation mechanism progressively reduces the model mismatch during iterative learning. This assumption does not require identical traffic and communication conditions in all trials, but requires their variations to be sufficiently smooth and estimable for the proposed learning framework.

2.3 ILC Task Description for Connected Vehicle Trajectory Tracking

For the repetitive connected-vehicle tracking task, the role of ILC is to improve the control input over repeated executions by using the tracking information obtained in previous trials. A general trial-to-trial update can be expressed as

$$u_{k+1} = F(u_k, e_k), \tag{10}$$

where the next input is adjusted according to the historical input and the current tracking error.

Based on the system model in (1), the control input for the next trial is determined by solving the following norm-optimal learning problem:

$$u_{k+1} = \arg\min_{u}\{\|y_d - G_{k+1}u - d_{k+1} - \varepsilon_{k+1}\|_Q^2 + \|u - u_k\|_R^2\}, \tag{11}$$

which produces the input sequence $\{u_k\}_{k\geq 0}$ together with the corresponding tracking-error sequence $\{e_k\}_{k\geq 0}$. The reference output is represented by y_d, and the tracking error in the k^{th} trial is given by

$$e_k = y_d - y_k, \tag{12}$$

$$y_d = G_d u_d + d_d, \tag{13}$$

where G_d and d_d are given by

$$G_d = \begin{bmatrix} \hat{\phi}_1\hat{\theta}_0 & 0 & \cdots & 0 \\ \hat{\phi}_2\hat{\varphi}_1\hat{\theta}_0 & \hat{\phi}_2\hat{\theta}_1 & \cdots & 0 \\ \vdots & \vdots & \ddots & \vdots \\ \hat{\phi}_N\prod_{j=1}^{N-1}\hat{\varphi}_j\hat{\theta}_0 & \hat{\phi}_N\prod_{j=2}^{N-1}\hat{\varphi}_j\hat{\theta}_1 & \cdots & \hat{\phi}_N\hat{\theta}_{N-1} \end{bmatrix}, \tag{14}$$

$$d_d = \begin{bmatrix} (\hat{\phi}_1\hat{\varphi}_0)^T, & (\hat{\phi}_2\hat{\varphi}_1\hat{\varphi}_0)^T, & \cdots, & (\hat{\phi}_N\prod_{j=0}^{N-1}\hat{\varphi}_j)^T \end{bmatrix}^T x_0. \tag{15}$$

The desired learning result is that the input sequence approaches the ideal input u_d and the tracking error converges to zero, namely

$$\lim_{k\to\infty} u_k = u_d, \qquad \lim_{k\to\infty} e_k = e^* = 0. \tag{16}$$

3 Parameter Estimation Solution

This section constructs the parameter-estimation component used in the proposed learning framework. The purpose is to obtain updated model information for connected vehicle trajectory tracking when traffic conditions, communication quality, and sensing measurements vary across trials. To support the subsequent estimation procedure, several probabilistic assumptions are introduced and then used to formulate the unified parameter update.

Although the proposed framework considers random noise, practical connected vehicle environments may involve stronger uncertainty sources, including communication interruptions, degraded sensing quality, and incomplete state observations. These factors may weaken the normality and Markov-type assumptions used in the estimator. In such situations, extended state observers or adaptive covariance-update mechanisms may be needed to improve estimation reliability.

Assumption 2: *Conditional observation independence assumption: once the current hidden state is specified, the observation at the current sampling instant is independent of other hidden states and past or future observations, i.e.*,

$$p(y_k(t)|x_k(1:N), y_k(1:t-1), y_k(t+1:N)) = p(y_k(t)|x_k(t)).$$

Assumption 3: *First-order homogeneous Markov assumption: the current hidden state is determined by the immediately preceding hidden state rather than by the complete state-observation history, i.e.*,

$$p(x_k(t)|x_k(1:t-1), y_k(1:t-1)) = p(x_k(t)|x_k(t-1)).$$

In repetitive trajectory-tracking tasks of connected vehicles, Assumption 2 is reasonable because the measured output at a given sampling instant is mainly determined by the current vehicle state and the local sensing or V2X measurement noise. Once the hidden state $x_k(t)$ is given, previous and future measurements influence the current observation only indirectly through state estimation. Therefore, the conditional independence structure provides a practical approximation for the observation process in the proposed estimation framework.

Assumption 3 follows from the discrete-time vehicle-motion model used in trajectory tracking. Under a sufficiently small sampling period, the current hidden state is mainly determined by the previous state, the applied control input, and the time-varying model parameters. Traffic variation, communication fluctuation, packet loss, and sensing uncertainty are incorporated into the time-varying parameters, disturbance term, or measurement noise rather than being modeled as long-memory processes. This Markov-type description is commonly used for finite-horizon vehicle control and enables recursive parameter estimation through Kalman-filter-based likelihood evaluation.

If severe traffic interactions, long communication outages, or unmodeled history-dependent disturbances dominate the system behavior, Assumptions 2 and 3 may only hold approximately. In such cases, the parameter estimates may fail to converge to their true values, and the ILC input may not fully compensate for the trial-varying dynamics. This limitation motivates the future use of extended observers or adaptive covariance-updating strategies for more complex connected-vehicle environments.

To describe the estimation process in a unified form, the time-varying parameter set is defined as

$$\Theta_t = \{\varphi_t, \theta_t, \phi_t\}, \tag{17}$$

where φ_t, θ_t, and ϕ_t denote the state, input, and output time-varying matrices, respectively. The corresponding estimate at the rth EM iteration is denoted by $\hat{\Theta}_t^{(r)} = \{\hat{\varphi}_t^{(r)}, \hat{\theta}_t^{(r)}, \hat{\phi}_t^{(r)}\}$. Given the input-output data collected from the kth trial, the posterior distribution of the unified parameter set can be factorized as

$$p(\Theta_t|y_k(1:N), u_k(0:N-1)) \propto p(y_k(1:N)|u_k(0:N-1), \Theta_t)p(\Theta_t), \tag{18}$$

where $p(\Theta_t)$ is the prior distribution of the parameter set. The likelihood term can be evaluated recursively by the Kalman filter as

$$p(y_k(1:N)|u_k(0:N-1), \Theta_t) = \prod_{i=1}^{N} p(y_k(i)|y_k(1:i-1), u_k(0:i-1), \Theta_t). \tag{19}$$

This unified representation enables the state-transition, input, and output matrices to be updated in the same iterative estimation process instead of being treated separately.

Based on the above probabilistic description, the parameter update is obtained through a maximum-likelihood estimation procedure.

Theorem 1: *The expectation maximization (EM) algorithm in [5] is applied to obtain the unified parameter-estimation sequence $\hat{\Theta}_t^{(r)}$ and find the optimal estimate $\hat{\Theta}_t^{*}$. The update at the $(r+1)$th EM iteration is given by*

$$\hat{\Theta}_t^{(r+1)} = \arg\max_{\Theta_t} \sum_{i=1}^{N} \mathbb{E}_{x_k(i)|y_k(1:N),u_k(0:N-1),\hat{\Theta}_t^{(r)}} \left[\log p(y_k(i), x_k(i)|u_k(i-1), \Theta_t)\right]. \tag{20}$$

Here, the expectation is taken with respect to the posterior distribution of the hidden state under the current parameter estimate $\hat{\Theta}_t^{(r)}$. The updated parameter set $\hat{\Theta}_t^{(r+1)}$ contains the estimates of φ_t, θ_t, and ϕ_t, which are then used to construct the lifted operators required by the ILC update.

Proof: The proof is provided in Appendix A. □

Under certain conditions on the likelihood-related functions $L(\Theta_t, \hat{\Theta}_t^{(r)})$ and $H(\Theta_t, \hat{\Theta}_t^{(r)})$, the convergence value $\hat{\Theta}_t^{*}$ of the unified parameter-estimation sequence obtained by Algorithm 1 is a stable point.

Algorithm 1: Unified time-varying parameter estimation for connected vehicle tracking

---

Input: Input-output data $\{u_k(i), y_k(i)\}_{i=1}^{N}$, initial state value $x(0)$, noise covariance matrices W_t and V_t, initial covariance $P(0)$, initial parameter estimate $\hat{\Theta}_t^{(0)}$, convergence tolerance δ_{EM}, and maximum EM iteration number $r_{\max}$.

Output: Estimated parameter set $\hat{\Theta}_t^{*} = \{\hat{\varphi}_t^{*}, \hat{\theta}_t^{*}, \hat{\phi}_t^{*}\}$ and the corresponding lifted operators G_k, d_k, and ε_k.

1: Initialize $r = 0$ and $\hat{\Theta}_t^{(0)} = \{\hat{\varphi}_t^{(0)}, \hat{\theta}_t^{(0)}, \hat{\phi}_t^{(0)}\}$.
2: **repeat**
3: E-step: use the Kalman filter recursion to compute the posterior distribution of the hidden state based on $\{u_k(i), y_k(i)\}_{i=1}^{N}$ and $\hat{\Theta}_t^{(r)}$.
4: M-step: update the unified parameter set $\hat{\Theta}_t^{(r+1)}$ by maximizing the expected complete-data log-likelihood in (20).
5: Set $r = r + 1$.
6: **until** $\|\hat{\Theta}_t^{(r)} - \hat{\Theta}_t^{(r-1)}\| \le \delta_{\mathrm{EM}}$ or $r = r_{\max}$
7: Set $\hat{\Theta}_t^{*} = \hat{\Theta}_t^{(r)}$ and construct G_k, d_k, and ε_k using $\hat{\varphi}_t^{*}$, $\hat{\theta}_t^{*}$, and $\hat{\phi}_t^{*}$.
8: **return** $\hat{\Theta}_t^{*}$, G_k, d_k, and ε_k.

The ILC framework proposed in Section 4 provides the input and observation data required by Algorithm 1, while Algorithm 1 supplies the unified estimates of φ_t, θ_t, and ϕ_t for constructing the lifted operators G_k, d_k, and ε_k. In this way, the parameter estimation mechanism and the ILC framework are integrated to support connected vehicle trajectory tracking under trial-varying traffic and communication conditions.

4 ILC Design Framework

This section develops the learning-control design based on the time-varying parameter estimates obtained in Section 3. The control update is first derived from a norm-optimal learning criterion, and the implementation procedure and convergence conditions are then presented.

4.1 Implementation of the Proposed Framework

The following cost function is introduced to determine the control input for the next trial:

$$J_{k+1} = ||e_{k+1}||_Q^2 + ||u_{k+1} - u_k||_R^2, \tag{21}$$

where e_{k+1} is obtained from the tracking-error definition in (12).

Theorem 2: *For the time-varying system in (1), minimizing the performance index in (21) leads to the learning update*

$$u_{k+1} = L_u u_k + L_e E_{(d,\varepsilon)}, \tag{22}$$

where L_u, L_e, and $E_{(d,\varepsilon)}$ are defined by

$$\begin{aligned} L_u &= (R + G_{k+1}^T Q G_{k+1})^{-1}(R + G_{k+1}^T Q G_k), \\ L_e &= (R + G_{k+1}^T Q G_{k+1})^{-1} G_{k+1}^T Q, \\ E_{(d,\varepsilon)} &= e_k - \Delta d_k - \Delta\varepsilon_k, \\ \Delta d_k &= d_{k+1} - d_k, \qquad \Delta\varepsilon_k = \varepsilon_{k+1} - \varepsilon_k. \end{aligned} \tag{23}$$

with $\Delta d_k = d_{k+1} - d_k$ and $\Delta\varepsilon_k = \varepsilon_{k+1} - \varepsilon_k$ representing the variations of the lifted bias term and the lifted noise/disturbance term between two consecutive trials, respectively. Since $d_k, d_{k+1}, \varepsilon_k, \varepsilon_{k+1} \in \mathbb{R}^{mN}$, it follows that $\Delta d_k, \Delta\varepsilon_k \in \mathbb{R}^{mN}$ and $E_{(d,\varepsilon)} \in \mathbb{R}^{mN}$.

Proof: The optimality condition of (11) is obtained by differentiating the quadratic performance index with respect to u_{k+1} under the weighted norm definition in (8). This gives

$$R(u_{k+1} - u_k) = G_{k+1}^T Q(y_d - G_{k+1}u_{k+1} - d_{k+1} - \varepsilon_{k+1}). \tag{24}$$

Using the tracking-error relation in (12) and the lifted system representation, the reference signal can be written as $y_d = G_k u_k + d_k + \varepsilon_k + e_k$. Substituting this relation into (11) gives the following equality:

$$\begin{aligned} &(R + G_{k+1}^T Q G_{k+1})u_{k+1} \\ &\quad = (R + G_{k+1}^T Q G_k)u_k + G_{k+1}^T Q E_{(d,\varepsilon)}. \end{aligned} \tag{25}$$

Because Q and R are symmetric positive definite matrices, $R + G_{k+1}^T Q G_{k+1}$ is invertible. Solving the above equation yields the update law in (22) with $L_e = (R + G_{k+1}^T Q G_{k+1})^{-1} G_{k+1}^T Q$, and the proof is completed. □

4.2 Algorithm Description

Algorithm 2 summarizes the proposed iterative learning procedure. It combines the parameter-estimation result generated by Algorithm 1 with the learning update in (22) to compute the control input for each new trial.

At each iteration, the estimated time-varying parameters are used to construct the lifted terms d_k and ε_k. The input u_{k+1} is then computed from (22) and applied to the system model in (1). After the system output y_{k+1} is obtained, the tracking error e_{k+1} is calculated and stored for the next learning update. This process is repeated until the maximum trial number $k_{\max}$ is reached.

In Algorithm 2, T_s denotes the sampling time, N denotes the number of sampling instants in each trial, and $k_{\max}$ denotes the maximum number of repeated trials. The initial lifted operators d_0 and ε_0 are the initial values of d_k and ε_k constructed from the lifted representation in Eqs. (4) and (5) at the initial trial.

Algorithm 2: ILC for connected vehicle trajectory tracking

Input: Desired reference trajectory y_d, initial input u_0, sampling time T_s, number of sampling instants N, maximum trial number $k_{\max}$, weighting matrices Q and R, and initial lifted operators d_0 and ε_0.
Output: Learned input sequence $\{u_k\}$ and tracking-error sequence $\{e_k\}$.
1: Set $k = 0$ and apply u_0 to system (1).
2: Record the output y_0 and compute the initial tracking error $e_0 = y_d - y_0$.
3: **for** $k = 0, 1, \cdots, k_{\max} - 1$ **do**
4: Estimate the time-varying parameter set $\hat{\Theta}_t^*$ using Algorithm 1.
5: Construct the lifted operators G_k, d_k, and ε_k according to the estimated parameters.
6: Compute u_{k+1} according to the ILC update law (22).
7: Apply u_{k+1} to system (1), record y_{k+1}, and compute $e_{k+1} = y_d - y_{k+1}$.
8: **end for**
9: **return** $\{u_k\}$ and $\{e_k\}$.

4.3 Convergence Analysis

The convergence property of Algorithm 2 is analyzed under two situations. The first situation considers the noise-free system, while the second one includes stochastic disturbance. This separation is adopted because the convergence mechanism of ILC differs when the repeated process is affected by noise.

a. Analysis for Noise-free Systems

The following lemma is used before deriving the noise-free convergence result.

Lemma 1: *For any matrix $A \in R^{m\times n}$ satisfying*

$$\gamma(A) < 1, \tag{26}$$

where $\gamma(A)$ denotes the spectral radius of A, the matrix A is convergent. In addition, there exists at least one matrix norm $||A||_S$ such that

$$\lim_{k\to\infty} ||A||_S^k = 0. \tag{27}$$

Proof: The proof is available in [26]. □

Theorem 3: *If*

$$||L_u - L_e G_k|| < \gamma < 1, \tag{28}$$

and

$$||G_d u_d|| + ||e_{d,k+1}|| \le \frac{(1-\gamma)||e_k||}{1-\gamma+||G_{k+1}||||L_e||}, \tag{29}$$

hold simultaneously, where $e_{d,k+1} = d_d - d_{k+1}$, then the tracking error converges.

Proof: The proof is given in Appendix B. □

b. Analysis for Noise-accompanied Systems

For the noise-accompanied case, the update law in (22) is examined under additional convexity and smoothness conditions. These conditions are used to establish a sufficient convergence result for the tracking error.

The error-related function $f(e_k)$ is treated as a convex function, and the associated optimization problem is assumed to satisfy the following boundedness and smoothness properties.

Assumption 4: *Function $f(e_k)$ has a lower bound and the strongly convex coefficient is Λ, and Ξ is the Lipschitz constant.*

The engineering rationale of Assumption 4 comes from the finite-horizon norm-optimal ILC formulation. The tracking objective and input-variation penalty are constructed with positive definite weighting matrices Q and R, so the corresponding optimization problem is lower bounded. In practical connected-vehicle trajectory tracking, the reference trajectory, input signal, and measured output are all confined to finite operating ranges. Under bounded time-varying parameter estimates, the gradient of the induced error-related function is Lipschitz continuous, and the local strong convexity condition can be satisfied around the admissible operating region. Therefore, Assumption 4 provides a tractable condition for establishing contraction-type convergence in the noisy case. If abrupt model switching or severe non-Gaussian disturbance occurs, this assumption may be weakened, and only local or practical convergence can be expected.

The following theorem presents a sufficient condition for convergence in the presence of noise.

In the following theorem, ρ is evaluated under the induced Q-weighted matrix norm

$$\|A\|_Q = \|Q^{1/2}AQ^{-1/2}\|_2. \tag{30}$$

Let $S_{k+1} = Q^{1/2}G_{k+1}R^{-1}G_{k+1}^TQ^{1/2}$. Then S_{k+1} is positive semidefinite because Q and R are symmetric positive definite. If S_{k+1} is positive definite on the considered tracking subspace, then

$$\rho = \left\|(I + G_{k+1}R^{-1}G_{k+1}^TQ)^{-1}\right\|_Q = \frac{1}{1+\lambda_{\min}(S_{k+1})}. \tag{31}$$

Therefore, $0 < \rho < 1$ holds when S_{k+1} is positive definite. Moreover, $\rho < 2/(\Lambda + \Xi)$ can be verified by checking $\lambda_{\min}(S_{k+1}) > \max\{0, (\Lambda + \Xi)/2 - 1\}$. Hence, the required interval of ρ is imposed through a verifiable eigenvalue condition under the selected matrix norm, rather than being inferred only from invertibility.

Theorem 4: *If the coefficients ρ and c satisfy*

$$\rho \in \left(0, min\left(1, \frac{2}{\Lambda + \Xi}\right)\right), \tag{32}$$

and

$$c \in (0,1), \tag{33}$$

where $\rho = \|(I + G_{k+1}R^{-1}G_{k+1}^TQ)^{-1}\|_Q$ and $c = 1 - \frac{2\rho\Xi\Lambda}{\Xi+\Lambda}$, then the tracking error e_k converges.

Proof: The proof is provided in Appendix C. □

5 Experimental Validation

This section validates the proposed method through a V2X-enabled connected vehicle trajectory-tracking framework. The experimental architecture and task configuration are first described, followed by parameter-estimation and tracking-performance comparisons.

5.1 V2X-Enabled Experimental Architecture and Tracking Task

The validation architecture is shown in Fig. 1. The framework contains four main parts: the traffic scenario, the V2X communication layer, the estimation and control layer, and the vehicle motion execution layer. The roadside unit, ego vehicle, and communication network are combined with the parameter-estimation and iterative-learning-control modules to reproduce connected-vehicle tracking tasks in repeated trials. Traffic variation, communication delay, packet loss, and measurement noise are included in the framework to emulate practical networked operating conditions. The estimated time-varying parameters are transmitted to the learning controller, and the measured motion output is fed back to the estimation and control modules through the sensing unit. In this way, a communication-in-the-loop closed-loop validation structure is formed.

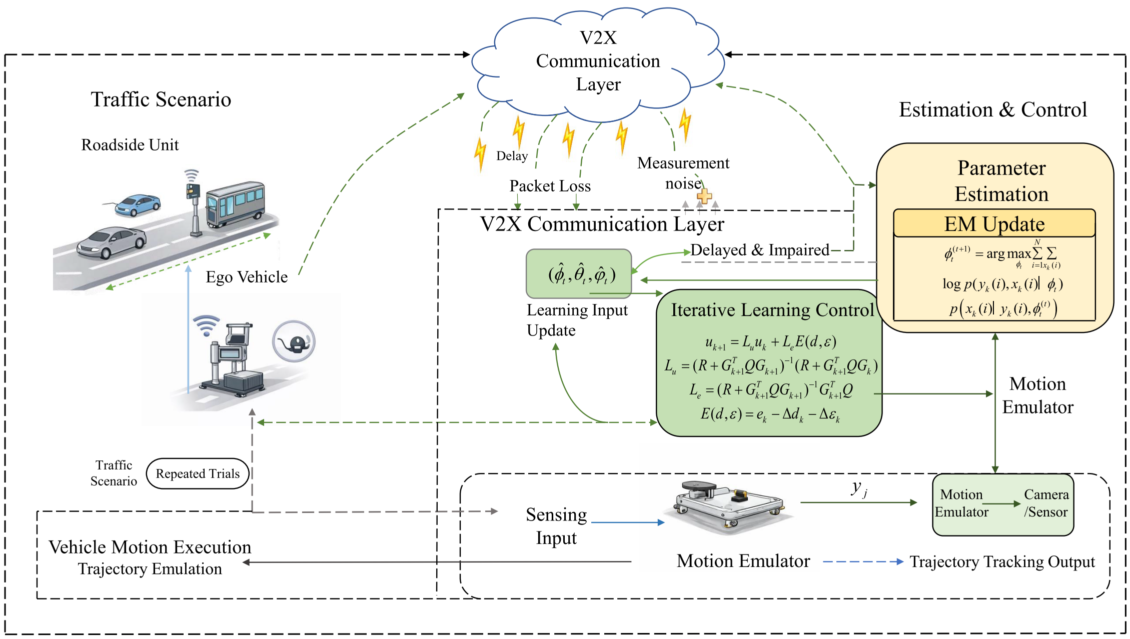

Figure 1: V2X-enabled experimental architecture for connected vehicle trajectory tracking.

For hardware emulation, the motion execution layer is implemented on an experimental platform that includes a gantry-type Cartesian motion mechanism, an industrial camera with a telecentric lens, a laser galvanometer, a two-dimensional rotary stage, and a precision sliding stage. The platform serves as a planar motion emulator for reproducing connected-vehicle trajectory-tracking behavior over repeated trials.

The feedback gains along the x-axis and y-axis are selected as 100 and −30, respectively. The discrete-time model uses the sampling time $T_s = 0.01$ s. The open-loop transfer function is written as

$$G_x = \frac{0.055z}{z-1}. \tag{34}$$

The duration of one repeated trial is chosen as $T = 2$. The desired reference trajectory y_d is specified by

$$\begin{aligned} &y_{d1} = [-1, 1],\ y_{d2} = [1, 1],\ y_{d3} = [2, 0], \\ &y_{d4} = [1, -1],\ y_{d5} = [-1, -1],\ y_{d6} = [-2, 0]. \end{aligned} \tag{35}$$

All algorithms were implemented in MATLAB under the same computational environment. The same sampling time, reference trajectory, initial input, weighting matrices, noise setting, and trial number were used for all compared methods to ensure a fair comparison. The maximum trial number was set to $k_{\max} = 80$. Unless otherwise specified, the weighting matrices in the comparison study were selected as $Q = 1{,}000{,}000I$ and $R = I$.

5.2 Parameter Estimation under Trial-Varying Traffic and Communication Conditions

Figs. 2–4 present the estimation results of the proposed mechanism under varying traffic, communication, and sensing conditions. The prior estimates show clear deviations from the ideal profiles, indicating the influence of network-induced perturbations and operating-condition changes on the connected vehicle model. After iterative estimation, the state, input, and output time-varying matrices move closer to their corresponding ideal values. The local enlarged regions further show that the final estimates provide improved local agreement, which indicates that the estimation module can capture the time-varying model characteristics and provide useful model information for the following ILC update.

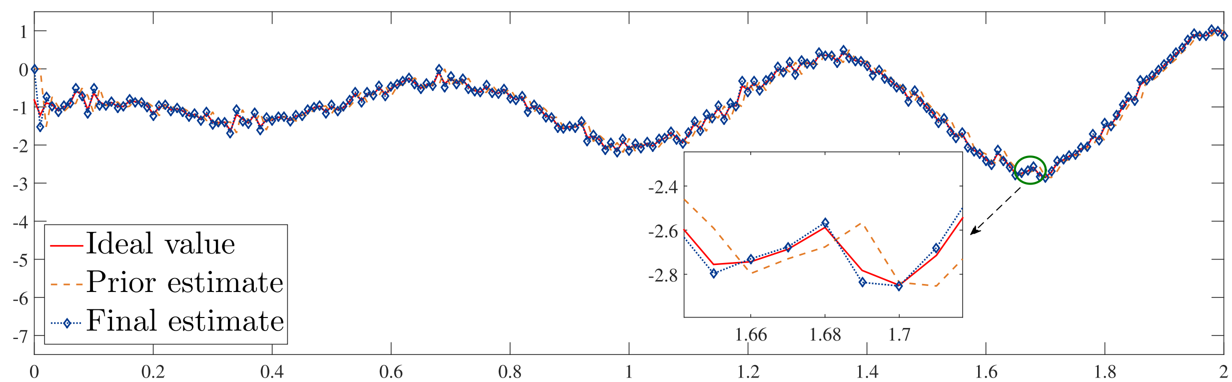

Figure 2: Estimation results of the state time-varying matrix φ_t under trial-varying traffic and communication conditions.

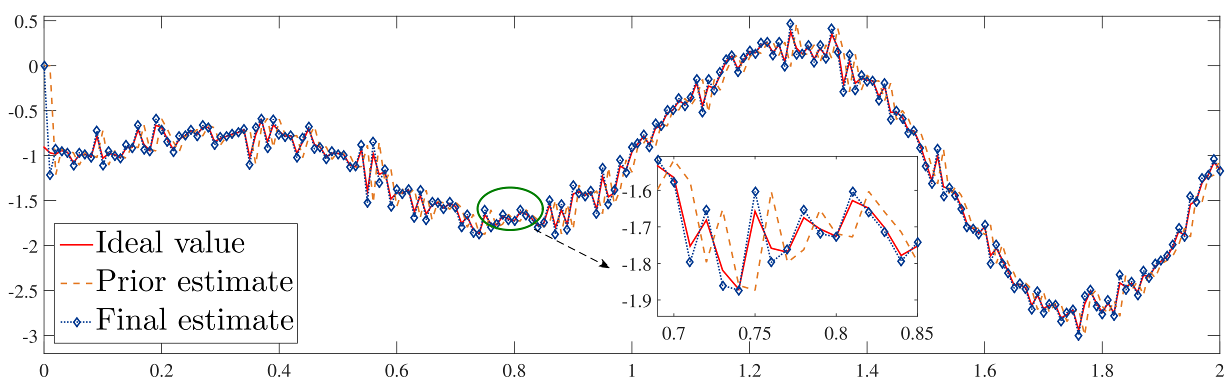

Figure 3: Estimation results of the input time-varying matrix θ_t under trial-varying traffic and communication conditions.

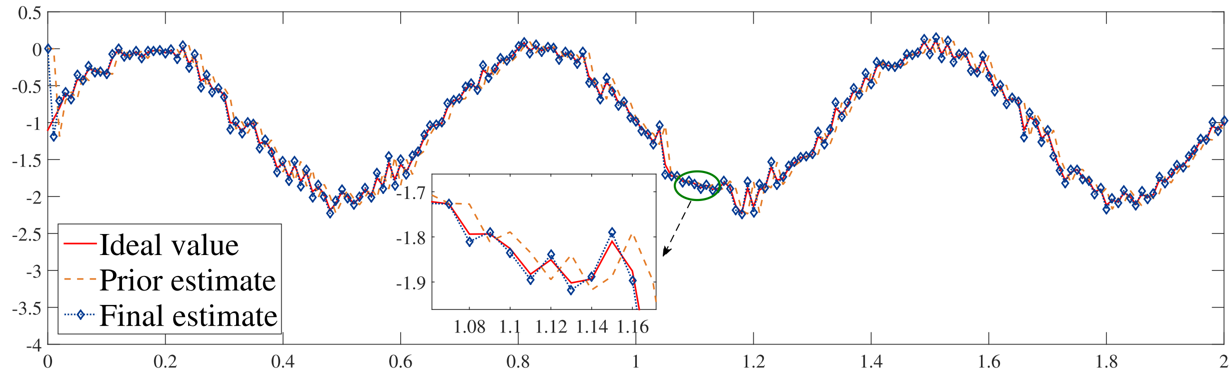

Figure 4: Estimation results of the output time-varying matrix ϕ_t under trial-varying traffic and communication conditions.

5.3 Tracking Performance under Trial-Varying Traffic and Communication Conditions

The tracking performance of the proposed method is tested over 80 repeated trials in the V2X-enabled connected vehicle trajectory-tracking framework. Fig. 5 reports the mean absolute tracking error for different weighting choices. In this comparison, R remains fixed, while Q is changed to examine how the weighting selection affects convergence and disturbance sensitivity under traffic variation, communication fluctuation, and sensing uncertainty. A larger Q usually leads to faster error reduction because the learning update gives more weight to tracking accuracy. However, an overly aggressive tracking weight may also increase sensitivity to network-induced mismatch and measurement perturbations. Therefore, the choice of Q should consider both convergence speed and robustness.

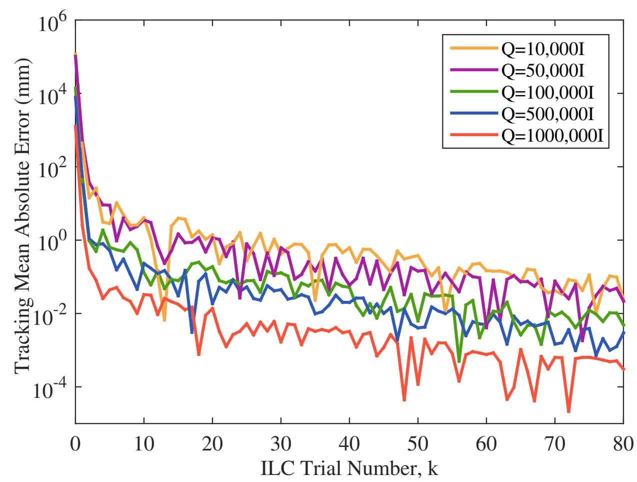

Figure 5: Mean absolute tracking-error curves for different weighting selections in the V2X-enabled connected vehicle trajectory-tracking task.

With Q = 1,000,000I and $R = I$, the proposed method is further compared with several representative baseline algorithms. In Fig. 6, ELM, ML, and BP denote the extreme learning machine, machine-learning-based, and backpropagation-neural-network-based estimation mechanisms, respectively, while RL denotes the reinforcement-learning-based adaptive control method. To make the comparison reproducible, the main parameter settings of the comparison algorithms are summarized in Table 1. All methods use the same desired trajectory, sampling time, trial number, initial condition, and noise profile. For the ILC-based comparison methods, the same norm-optimal ILC update structure is adopted, while the parameter-estimation module is replaced by the corresponding estimation mechanism.

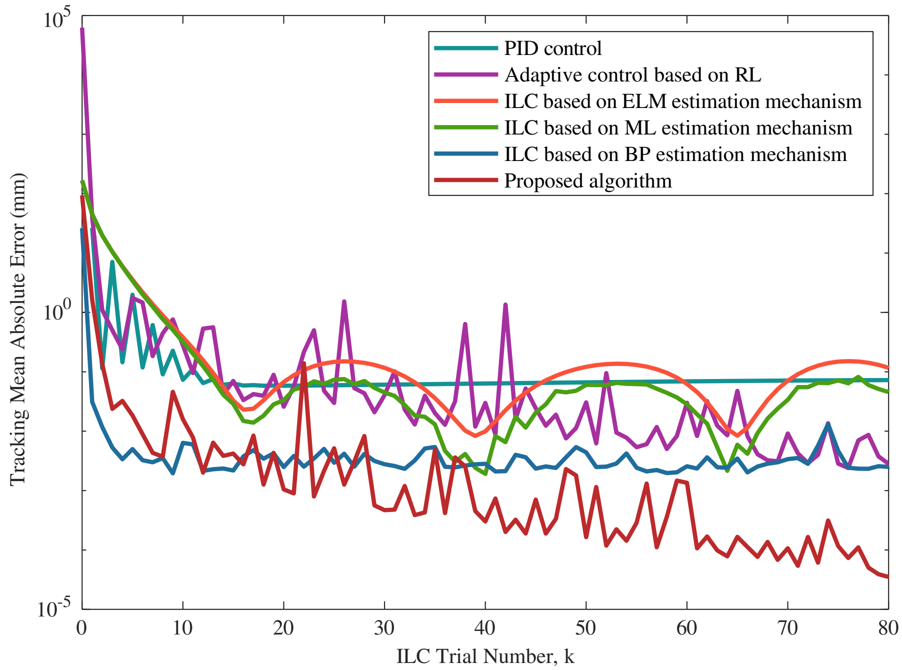

Figure 6: Comparison of tracking mean absolute errors under trial-varying traffic and communication conditions.

Table 1: Parameter settings of the comparison algorithms.

Algorithm	Main Parameter Settings
PID control	The feedback gains in the x-axis and y-axis directions were chosen as 100 and −30, respectively. This method used the same desired trajectory and initial condition, but did not include a trial-to-trial learning update.
Adaptive control based on RL	The learning rate, discount factor, and exploration probability were set as $\alpha_{\mathrm{RL}} = 0.01$, $\gamma_{\mathrm{RL}} = 0.95$, and $\varepsilon_{\mathrm{RL}} = 0.05$, respectively. The reward function was defined according to the tracking error and the input variation.
ILC based on ELM estimation	The ELM estimator adopted a single hidden layer with 50 hidden neurons, a sigmoid activation function, and the regularization coefficient 10^{-6}. The estimated parameters were then inserted into the same ILC update law.
ILC based on ML estimation	Parameter regression was performed using the same input-output data. The regularization coefficient was chosen as 10^{-4}, and the resulting time-varying parameter estimates were used to build the lifted operators for the ILC update.
ILC based on BP estimation	The BP neural network used one hidden layer with 20 neurons. The learning rate was 0.01, the maximum number of training epochs was 500, and the mean-square-error stopping tolerance was 10^{-6}.

(Continued)

Table 1 (continued)

Algorithm	Main Parameter Settings
Proposed algorithm	The proposed method adopted the unified EM-based estimator with the convergence tolerance $\delta_{\mathrm{EM}} = 10^{-6}$ and the maximum EM iteration number $r_{\max} = 50$. The estimated parameter set $\hat{\Theta}_t^*$ was used to construct G_k, d_k, and ε_k for the ILC update.

In addition to the tracking mean absolute error comparison, three quantitative indices are used to further evaluate the compared algorithms. The single-trial computation time reflects the CPU time required to complete one online control or learning update within a single trial. The convergence iteration number reflects the number of learning trials required to reach a stable low-error region. The average computation time evaluates the total online computational burden required to reach convergence. For methods that do not show visible convergence within 80 repeated trials, the average computation time required for convergence is marked by "–". The quantitative comparison results are summarized in Table 2.

Table 2: Numerical comparison of benchmark methods under trial-varying traffic and communication conditions.

Algorithm	Single-Trial Comp. Time (s)	Conv. Iter.	Avg. Computation Time (s)
PID control	0.002	>80	–
Adaptive control based on RL	0.015	>80	–
ILC based on ELM estimation	0.008	65	0.520
ILC based on ML estimation	0.006	60	0.360
ILC based on BP estimation	0.010	17	0.170
Proposed algorithm	0.007	35	0.245

In Table 2, >80 indicates that the corresponding method does not show visible convergence within 80 repeated trials, and "–" indicates that the average computation time required for convergence is not reported because visible convergence is not achieved within the trial range. PID control has the lowest single-trial computation time, but it does not show visible convergence within 80 trials. The RL-based adaptive control method also fails to show visible convergence within 80 trials and requires a larger single-trial computation time than PID control. The ELM- and ML-estimation-based ILC methods converge after 65 and 60 trials, respectively, but require relatively larger average computation times. The BP-estimation-based ILC method reaches convergence after 17 trials and requires an average computation time of 0.170 s. The proposed algorithm converges after 35 trials with an average computation time of 0.245 s, indicating a moderate online computational burden while maintaining stable learning performance under trial-varying traffic and communication conditions.

Figs. 7 and 8 show the trajectory evolution under nominal and perturbed operating conditions, respectively. Fig. 7 gives the result without network-induced disturbance. The output trajectory approaches the desired trajectory y_d as the number of trials increases. Fig. 8 gives the result with disturbance, which reflects the combined influence of communication fluctuation and sensing noise in the V2X-enabled connected vehicle scenario. The initial trial has a visible deviation from the desired trajectory. After repeated learning updates, the trajectory moves toward y_d, showing that the proposed method can maintain acceptable tracking performance under perturbed networked conditions.

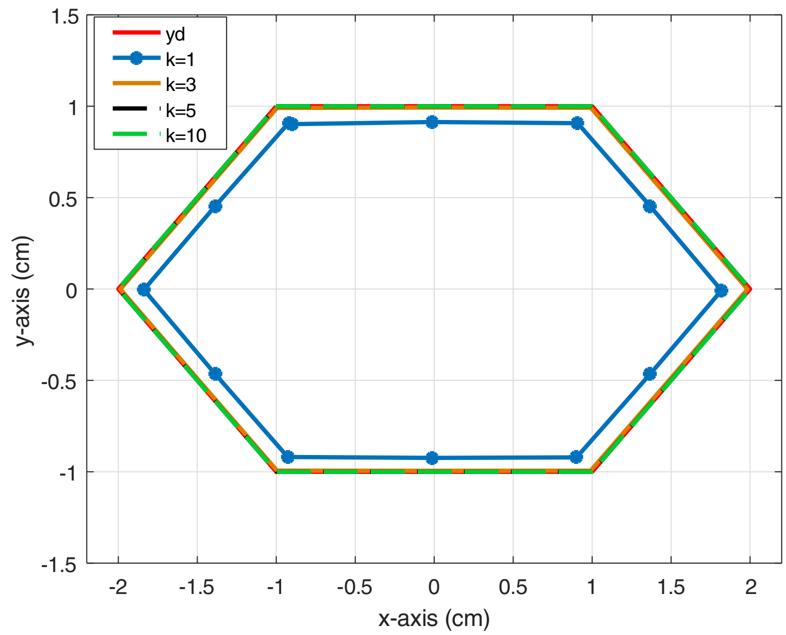

Figure 7: Tracking trajectories under nominal communication and sensing conditions.

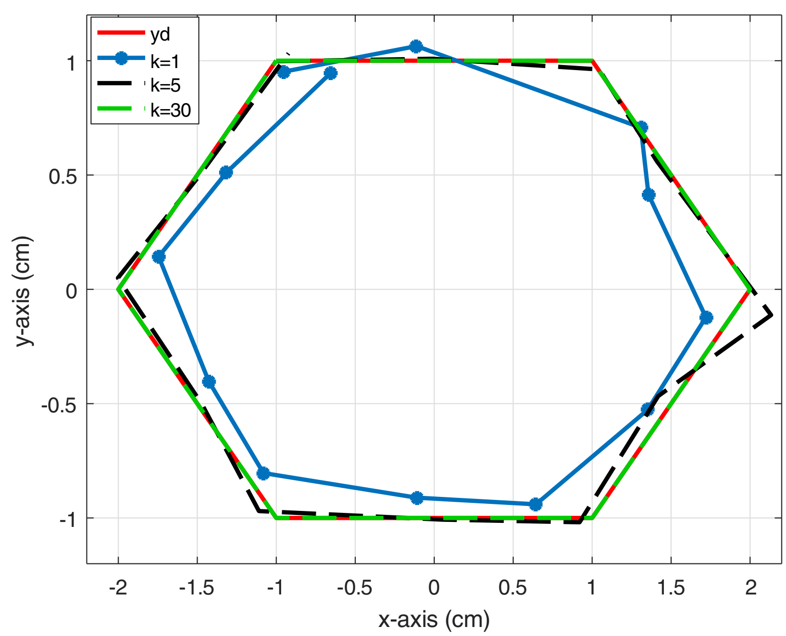

Figure 8: Tracking trajectories under perturbed communication and sensing conditions.

6 Conclusion and Future Work

This study has developed a parameter-estimation-based iterative learning control scheme for repetitive trajectory tracking of connected vehicles under trial-varying traffic and communication conditions. The expectation-maximization estimation mechanism has been embedded into the ILC framework to update the time-varying model information and the learning input during repeated trials. The proposed design has addressed the influence of traffic variation, communication fluctuation, and sensing uncertainty on tracking performance. Simulation results within the V2X-enabled validation framework have shown that the proposed method improves tracking precision and convergence behavior compared with the benchmark algorithms.

Future research will focus on several extensions. Input constraints will be included to enhance practical applicability. The robustness of the method under stronger model uncertainty, communication degradation, and sensing disturbances will be further analyzed. In addition, performance optimization will be studied for more complex V2X-enabled connected-vehicle trajectory-tracking scenarios.

Acknowledgement: None.

Funding Statement: This work was supported by the Natural Science Foundation of the Jiangsu Higher Education Institutions of China (No. 25KJB120011) and Wuxi University Research Start-up Fund for High-level Talents (No. 2025r011).

Author Contributions: Investigation, writing, methodology and experiments, Ping Ma; conceptualization, software and formal analysis, Yiyang Chen; validation and supervision, Quan Wang. All authors reviewed and approved the final version of the manuscript.

Availability of Data and Materials: The data that support the findings of this study are available from the Corresponding Author, Yiyang Chen, upon reasonable request.

Ethics Approval: This study did not involve any human or animal subjects, and therefore, ethical approval was not required.

Conflicts of Interest: The authors declare no conflicts of interest.

Appendix A Proof of Theorem 1

For consistency with the unified parameter-estimation framework in Section 3, the proof is rewritten by using the unified parameter set $\Theta_t = \{\varphi_t, \theta_t, \phi_t\}$. Let $\hat{\Theta}_t^{(r)}$ and $\hat{\Theta}_t^{(r+1)}$ denote two consecutive EM estimates. For notational compactness, define

$$\mathcal{D}_k = \{y_k(1:N), u_k(0:N-1)\}, \quad \mathcal{Y}_i^- = y_k(1:i-1), \quad \mathcal{U}_i^- = u_k(0:i-1). \tag{A1}$$

The observed-data log-likelihood is written as

$$\ell(\Theta_t) = \sum_{i=1}^{N} \log p\big(y_k(i) \mid \mathcal{Y}_i^-, \mathcal{U}_i^-, \Theta_t\big). \tag{A2}$$

The posterior distribution of the hidden state under the current estimate is denoted by

$$q_i^{(r)}(x_k(i)) = p\big(x_k(i) \mid \mathcal{D}_k, \hat{\Theta}_t^{(r)}\big). \tag{A3}$$

For continuous hidden states, the summation over $x_k(i)$ can be replaced by the corresponding integral.

Then, the expected complete-data log-likelihood is defined as

$$\begin{aligned} L(\Theta_t, \hat{\Theta}_t^{(r)}) = \sum_{i=1}^{N} \sum_{x_k(i)} & q_i^{(r)}(x_k(i)) \\ & \times \log p\big(y_k(i), x_k(i) \mid u_k(i-1), \Theta_t\big). \end{aligned} \tag{A4}$$

The corresponding posterior-related term is defined as

$$H(\Theta_t, \hat{\Theta}_t^{(r)}) = \sum_{i=1}^{N} \sum_{x_k(i)} q_i^{(r)}(x_k(i)) \times \log p\big(x_k(i) \mid \mathcal{D}_k, \Theta_t\big). \tag{A5}$$

According to the standard EM decomposition, the observed-data log-likelihood satisfies

$$\ell(\Theta_t) = L(\Theta_t, \hat{\Theta}_t^{(r)}) - H(\Theta_t, \hat{\Theta}_t^{(r)}). \tag{A6}$$

Taking $\hat{\Theta}_t^{(r+1)}$ and $\hat{\Theta}_t^{(r)}$ in the above relation yields

$$\begin{aligned}&\ell(\hat{\Theta}_t^{(r+1)}) - \ell(\hat{\Theta}_t^{(r)}) \\ &\quad= \Big[L(\hat{\Theta}_t^{(r+1)}, \hat{\Theta}_t^{(r)}) - L(\hat{\Theta}_t^{(r)}, \hat{\Theta}_t^{(r)})\Big] \\ &\quad- \Big[H(\hat{\Theta}_t^{(r+1)}, \hat{\Theta}_t^{(r)}) - H(\hat{\Theta}_t^{(r)}, \hat{\Theta}_t^{(r)})\Big].\end{aligned} \tag{A7}$$

From the M-step in Eq. (20), $\hat{\Theta}_t^{(r+1)}$ maximizes the expected complete-data log-likelihood. Therefore,

$$L(\hat{\Theta}_t^{(r+1)}, \hat{\Theta}_t^{(r)}) - L(\hat{\Theta}_t^{(r)}, \hat{\Theta}_t^{(r)}) \geq 0. \tag{A8}$$

Furthermore, by Jensen's inequality [27],

$$\begin{aligned}&H(\hat{\Theta}_t^{(r+1)}, \hat{\Theta}_t^{(r)}) - H(\hat{\Theta}_t^{(r)}, \hat{\Theta}_t^{(r)}) \\ &\quad= \sum_{i=1}^{N} \sum_{x_k(i)} q_i^{(r)}(x_k(i)) \log \frac{p\big(x_k(i) \mid \mathcal{D}_k, \hat{\Theta}_t^{(r+1)}\big)}{q_i^{(r)}(x_k(i))} \\ &\quad\leq \sum_{i=1}^{N} \log\left[\sum_{x_k(i)} p\big(x_k(i) \mid \mathcal{D}_k, \hat{\Theta}_t^{(r+1)}\big)\right] = 0.\end{aligned} \tag{A9}$$

Combining the above two inequalities gives

$$\ell(\hat{\Theta}_t^{(r+1)}) - \ell(\hat{\Theta}_t^{(r)}) \geq 0. \tag{A10}$$

Thus, the observed-data log-likelihood is nondecreasing during the EM iterations. Under the regularity and boundedness conditions of the EM procedure, the unified parameter-estimation sequence approaches a stable point $\hat{\Theta}_t^*$. Since Θ_t contains φ_t, θ_t, and ϕ_t, the proof is consistent with the unified multi-parameter estimation framework used in Theorem 1 and Algorithm 1.

Appendix B Proof of Theorem 3

Consider the system dynamics without noise, then the update law becomes

$$u_{k+1} = L_u u_k + L_e E_d, \tag{A11}$$

where $E_d = e_k - \Delta d_k$. Substituting (12) and (13) into E_d gives

$$E_d = G_d u_d - G_k u_k + d_d - d_{k+1}, \tag{A12}$$

where $d_d - d_{k+1}$ is written as $e_{d,k+1}$. The update law (A11) converts to the following form

$$u_{k+1} = (L_u - L_e G_k)u_k + L_e G_d u_d + L_e e_{d,k+1}, \tag{A13}$$

in which L_u and L_e are the same as that in (22).

Take the norm for both sides of the above formula to give

$$||u_{k+1}|| = ||(L_u - L_e G_k)u_k + L_e G_d u_d + L_e e_{d,k+1}||, \tag{A14}$$

and the inequality with respect to $||u_{k+1}||$ holds as follows:

$$||u_{k+1}|| \leq ||L_u - L_e G_k||||u_k|| + ||L_e||||G_d u_d|| + ||L_e||||e_{d,k+1}||. \tag{A15}$$

Induction on (A15), there exists

$$\begin{aligned} ||u_{k+1}|| &\leq ||L_u - L_e G_k||^{k+1}||u_0|| \\ &+ \frac{1 - ||L_u - L_e G_k||^{k+1}}{1 - ||L_u - L_e G_k||}(||L_e||||G_d u_d|| + ||L_e||||e_{d,k+1}||). \end{aligned} \tag{A16}$$

By Lemma 1, if $||L_u - L_e G_k|| < \gamma < 1$ holds, there exists

$$\lim_{k\to\infty} ||L_u - L_e G_k||^k = 0, \tag{A17}$$

then the inequality about $||u_{k+1}||$ turns into

$$||u_{k+1}|| \leq \frac{1}{1-\gamma}(||L_e||||G_d u_d|| + ||L_e||||e_{d,k+1}||). \tag{A18}$$

On the basis of (12), the norm of error for $(k+1)$ trial satisfies

$$||e_{k+1}|| \leq ||G_d u_d|| + ||G_{k+1}||||u_{k+1}|| + ||e_{d,k+1}||. \tag{A19}$$

The norm inequality with respect to u_{k+1} is substituted to obtain

$$||e_{k+1}|| \leq (\frac{||G_{k+1}||||L_e||}{1-\gamma} + 1)(||G_d u_d|| + ||e_{d,k+1}||). \tag{A20}$$

If the inequality (29) satisfies, the convergence analysis is validated, which finishes the proof.

Appendix C Proof of Theorem 4

The error for the $(k+1)$th trial can be written in another form by minimizing (21) with respect to u_{k+1} as

$$e_{k+1} = \rho e_k - \rho \nabla f(e_k), \tag{A21}$$

where $\rho = \|(I + G_{k+1}R^{-1}G_{k+1}^T Q)^{-1}\|_Q$ is evaluated under the induced Q-weighted norm and $\nabla f(e_k) = \Delta G_k u_k + \Delta d_k + \Delta \varepsilon_k$.

Define $g(e_k) \triangleq f(e_k) - \frac{\Lambda e_k^T e_k}{2}$. Since $f(e_k)$ is differentiable, differentiating $g(e_k)$ gives

$$\nabla g(e_k) = \nabla f(e_k) - \Lambda e_k. \tag{A22}$$

From Assumption 4 and the properties of convex functions, $g(e_k)$ and $h(e_k) \triangleq \frac{\Xi-\Lambda}{2}e_k^T e_k - g(e_k)$ are convex. According to the co-coercivity property of differentiable convex functions with Lipschitz-continuous gradients [28], the following inequality holds:

$$[\nabla g(x) - \nabla g(y)]^T(x-y) \geq \frac{1}{\Xi - \Lambda}\|\nabla g(x) - \nabla g(y)\|^2. \tag{A23}$$

Substituting (A22) into the above inequality yields

$$\begin{aligned}&[\nabla f(x) - \nabla f(y)]^T(x-y) - \Lambda\|x-y\|^2\\ &\quad\geq \frac{1}{\Xi-\Lambda}\left(\|\nabla f(x) - \nabla f(y)\|^2 + \Lambda^2\|x-y\|^2\right)\\ &\quad-\frac{2\Lambda}{\Xi-\Lambda}[(\nabla f(x) - \nabla f(y))^T(x-y)].\end{aligned} \tag{A24}$$

Then, the following inequality is obtained:

$$\begin{aligned}&[\nabla f(x) - \nabla f(y)]^T(x-y)\\ &\quad\geq \frac{1}{\Xi+\Lambda}\|\nabla f(x) - \nabla f(y)\|^2 + \frac{\Xi\Lambda}{\Xi+\Lambda}\|x-y\|^2.\end{aligned} \tag{A25}$$

In the next step, an error inequality is constructed to prove convergence. Since the desired error satisfies $e^* = 0$, it follows from (A21) that

$$\|e_{k+1}\|^2 = \|\rho e_k - \rho e^*\|^2 - 2\rho\nabla f(e_k)^T(e_k - e^*) + \rho^2\|\nabla f(e_k)\|^2. \tag{A26}$$

Using the inequality in (A25) with $x = e_k$ and $y = e^*$ gives

$$\begin{aligned}&\|e_{k+1} - \rho e^*\|^2 \leq \|\rho e_k - \rho e^*\|^2 - \frac{2\rho}{\Xi+\Lambda}\|\nabla f(e_k)\|^2\\ &\quad-\frac{2\rho\Xi\Lambda}{\Xi+\Lambda}\|e_k - e^*\|^2 + \rho^2\|\nabla f(e_k)\|^2.\end{aligned} \tag{A27}$$

If condition (32) is satisfied, the coefficient of $\|\nabla f(e_k)\|^2$ is non-positive. Therefore, the above inequality becomes

$$\|e_{k+1} - \rho e^*\|^2 \leq \|\rho e_k - \rho e^*\|^2 - \frac{2\rho\Xi\Lambda}{\Xi+\Lambda}\|e_k - e^*\|^2. \tag{A28}$$

The interval of ρ is justified under the induced Q-weighted norm defined in Section 4.3. Let

$$S_{k+1} = Q^{1/2}G_{k+1}R^{-1}G_{k+1}^TQ^{1/2}. \tag{A29}$$

Since Q and R are symmetric positive definite matrices, S_{k+1} is positive semidefinite. When S_{k+1} is positive definite on the considered tracking subspace and satisfies $\lambda_{\min}(S_{k+1}) > \max\{0, (\Lambda+\Xi)/2 - 1\}$, one has

$$\begin{aligned}\rho &= \left\|(I + G_{k+1}R^{-1}G_{k+1}^TQ)^{-1}\right\|_Q\\ &= \left\|(I+S_{k+1})^{-1}\right\|_2 = \frac{1}{1+\lambda_{\min}(S_{k+1})}.\end{aligned} \tag{A30}$$

Hence, $\rho \in (0, \min(1, 2/(\Lambda + \Xi)))$ is obtained under the selected matrix norm rather than from invertibility alone. Since $\rho < 1$, the preceding inequality can be further bounded as

$$\|e_{k+1} - \rho e^*\|^2 \le \left(1 - \frac{2\rho\Xi\Lambda}{\Xi + \Lambda}\right)\|e_k - e^*\|^2. \tag{A31}$$

where $c = 1 - \frac{2\rho\Xi\Lambda}{\Xi+\Lambda}$ is defined. Together with condition (33), one has $c \in (0, 1)$. Therefore, the tracking error sequence $\{e_k\}$ is contractive in the noisy case, which completes the proof.

References

1. Zhang X, Li J, Zhou J, Zhang S, Wang J, Yuan Y, et al. Vehicle-to-everything communication in intelligent connected vehicles: a survey and taxonomy. Automot Innov. 2025;8(1):13–45. doi:10.1007/s42154-024-00310-2.
2. Clancy J, Mullins D, Deegan B, Horgan J, Ward E, Eising C, et al. Wireless access for V2X communications: research, challenges and opportunities. IEEE Commun Surv Tutor. 2024;26(3):2082–119.
3. Long K, Ma K, Li Q, Li X, Huang Z, James R, et al. A comprehensive assessment of connected and automated vehicle analytical, modeling, and simulation tools. Transp Res Part E Logist Transp Rev. 2025;196:104007. doi:10.1016/j.tre.2025.104007.
4. Gaudio JE, Annaswamy AM, Lavretsky E, Bolender MA. Parameter estimation in adaptive control of time-varying systems under a range of excitation conditions. IEEE Trans Autom Control. 2022;67(10):5440–7. doi:10.1109/tac.2021.3126243.
5. Elvira V, Chouzenoux E. Graphical inference in linear-gaussian state-space models. IEEE Trans Signal Process. 2022;70(12):4757–71. doi:10.1109/tsp.2022.3209016.
6. Li W, Zhu T, Feng Y. A cooperative perception based adaptive signal control under early deployment of connected and automated vehicles. Transp Res Part C Emerg Technol. 2024;169(9):104860. doi:10.1016/j.trc.2024.104860.
7. Wang Q, Ye G, Li F, Chen Q, Jiang J, Zhang S, et al. YOLO-LIGHT: a real-time lightweight model based on limited edge computing for traffic scene detection and tracking. IEEE Trans Intell Transp Syst. 2026;27(6):6874–89.
8. Ma W, Chen B, Yu C, Qi X. Trajectory planning for connected and autonomous vehicles at freeway work zones under mixed traffic environment. Transp Res Rec. 2022;2676(10):207–19. doi:10.1177/03611981221088766.
9. Hu Y, Wang Y, Guo J, Zhang L, Lu Q, Liu H, et al. Eco-driving of connected autonomous vehicles in urban traffic networks of mixed autonomy with cut-in and escape lane-changes of manually-driven vehicles. Transp Res Part C: Emerg Technol. 2024;169(2):104889. doi:10.1016/j.trc.2024.104889.
10. Yao S, Zhou Y, Friedrich B, Ahn S. Planning trajectories for connected and automated vehicle platoons under mixed traffic conditions in complex road geometry. Transp Res Part C Emerg Technol. 2024;165(4):104718. doi:10.1016/j.trpro.2020.03.089.
11. Liu M, Gao Y, Zeng Y, Hao R. Distributed trajectory optimization for connected and automated vehicle platoons considering safe inter-vehicle following gaps. Systems. 2025;13(6):483. doi:10.3390/systems13060483.
12. Gu X, Wu Q, Fan P, Fan Q, Cheng N, Chen W, et al. DRL-based resource allocation for motion blur resistant federated self-supervised learning in IoV. IEEE Internet Things J. 2025;12(6):7076–85. doi:10.1109/jiot.2024.3492326.
13. Xie Y, Wu Q, Fan P, Cheng N, Chen W, Wang J, et al. Resource allocation for twin maintenance and task processing in vehicular edge computing network. IEEE Internet Things J. 2025;12(15):32008–21. doi:10.1109/jiot.2025.3576582.
14. Zhang Z, Wu Q, Fan P, Cheng N, Chen W, Letaief KB. DRL-based optimization for AoI and energy consumption in C-V2X enabled IoV. IEEE Trans Green Commun Netw. 2025;9(4):2144–59. doi:10.1109/tgcn.2025.3531902.
15. Chen Y, Chu B, Freeman CT. Iterative learning control for robotic path following with trial-varying motion profiles. IEEE/ASME Trans Mechatron. 2022;27(6):4697–706. doi:10.1109/tmech.2022.3164101.
16. Bu X, Yu W, Yu Q, Hou Z, Yang J. Event-triggered model-free adaptive iterative learning control for a class of nonlinear systems over fading channels. IEEE Trans Cybern. 2022;52(9):9597–608. doi:10.1109/tcyb.2021.3058997.
17. Liang M, Li J, Li J. Coordinated fuzzy adaptive iterative learning control of consensus for unknown nonlinear multi-agent systems. Int J Fuzzy Syst. 2022;24(6):3000–14. doi:10.1007/s40815-022-01317-9.

18. Liu L, Liu H, Ding F, Alsaedi A, Hayat T. Data filtering based maximum likelihood gradient estimation algorithms for a multivariate equation-error system with ARMA noise. J Frankl Inst. 2020;357(9):5640–62. doi:10.1016/j.jfranklin.2020.03.047.
19. Xia H, Wu Z, Xu S, Liu L, Li Y, Zhou Y. Auxiliary model-based interval-varying maximum likelihood estimation for nonlinear systems with missing data. Int J Robust Nonlinear Control. 2024;34(2):1312–23. doi:10.1002/rnc.7031.
20. Liu J, Zheng Y, Chen Y. Monotonically convergent iterative learning control by time varying learning gain revisited. Automatica. 2023;157(6):111259. doi:10.1016/j.automatica.2023.111259.
21. Wang L, Huangfu Z, Li R, Wen X, Sun Y, Chen Y. Iterative learning control with parameter estimation for non-repetitive time-varying systems. J Frankl Inst. 2024;361(3):1455–66. doi:10.1016/j.jfranklin.2024.01.011.
22. Chi R, Hou Z, Jin S, Wang D. Improved data-driven optimal TILC using time-varying input signals. J Process Control. 2014;24(12):78–85. doi:10.1016/j.jprocont.2014.07.007.
23. Owens DH, Freeman CT, Van Dinh T. Norm-optimal iterative learning control with intermediate point weighting: theory, algorithms, and experimental evaluation. IEEE Trans Control Syst Technol. 2013;21(3):999–1007. doi:10.1109/tcst.2012.2196281.
24. Shen D, Xu JX. An iterative learning control algorithm with gain adaptation for stochastic systems. IEEE Trans Autom Control. 2020;65(3):1280–7. doi:10.1109/tac.2019.2925495.
25. Shen D. Iterative learning control using faded measurements without system information: a gradient estimation approach. Int J Syst Sci. 2020;51(2):2675–89. doi:10.1080/00207721.2020.1799258.
26. Yang S, Xu JX, Huang D, Tan Y. Optimal iterative learning control design for multi-agent systems consensus tracking. Syst Control Lett. 2014;69(1):80–9. doi:10.1016/j.sysconle.2014.04.009.
27. Yokoyama N. Parameter estimation of aircraft dynamics via unscented smoother with expectation- maximization algorithm. J Guid Control Dyn. 2011;34(2):426–36. doi:10.2514/1.51696.
28. Bauschke HH, Combettes PL. The baillon-haddad theorem revisited. J Convex Anal. 2010;17(3–4):781–7. doi:10.48550/arxiv.0906.0807.